PHOENICS Newsletter

CHAM

Dear Reader

January 09 2023 marks Brian Spalding's 100th Birthday. He will be remembered in a special edition of the PHOENICS Newsletter containing memories from:

1) *Those who knew him scientifically;*
2) *Those who knew him personally;*
3) *Or both*

We hope to remember scientist, academic, mentor, free thinker, father of CFD, creator of PHOENICS, poet, intellectual and much more. We are seeking contributions which are brief "snapshots" reflecting the person. Did you meet Brian at a Conference? Was he your PhD supervisor? Did you read his work and find it influential? Please send your memories.

Contributions will reflect a man who made a major impact on many aspects of life for 70 years. Please send items to: newsletter@cham.co.uk. We welcome photos of Brian with you, in a group, anywhere; plus tapes, CDs, videos, any record of him speaking which could be shared on our website.

I look forward to hearing from you.

Kind regards

Colleen Spalding

Contents

Concentration, Heat and Momentum Limited (CHAM)
Bakery House, 40 High Street, Wimbledon Village, London, SW19 5AU, England
Tel: +44 (0)20 8947 7651 Email: phoenics@cham.co.uk Web: www.cham.co.uk

Autumn 2022

In PHOENICS-2022 the convergence monitor screen displayed by the Earth solver has a more modern, flexible, feel.

The tabs display, as a function of sweep:

- **'CMD'** - text output from the solver
- **'Spot value'** - values of all variables at the selected monitor point
- **'Global Maximums'** - largest value in the domain
- **'Global Minimums'** - smallest value in the domain
- **'Residual'** - the normalised sum of errors for each variable
- **'Net Sources'** - net sum of sources for all variables.
- **'Max Correction'** – largest correction between iterations

Each tab can be displayed by clicking the tab header. Alternatively, the tabs can be pulled out to make individual windows. In this way all six plots can be displayed simultaneously. Here, all the individual tabs have been pulled out into separate windows:

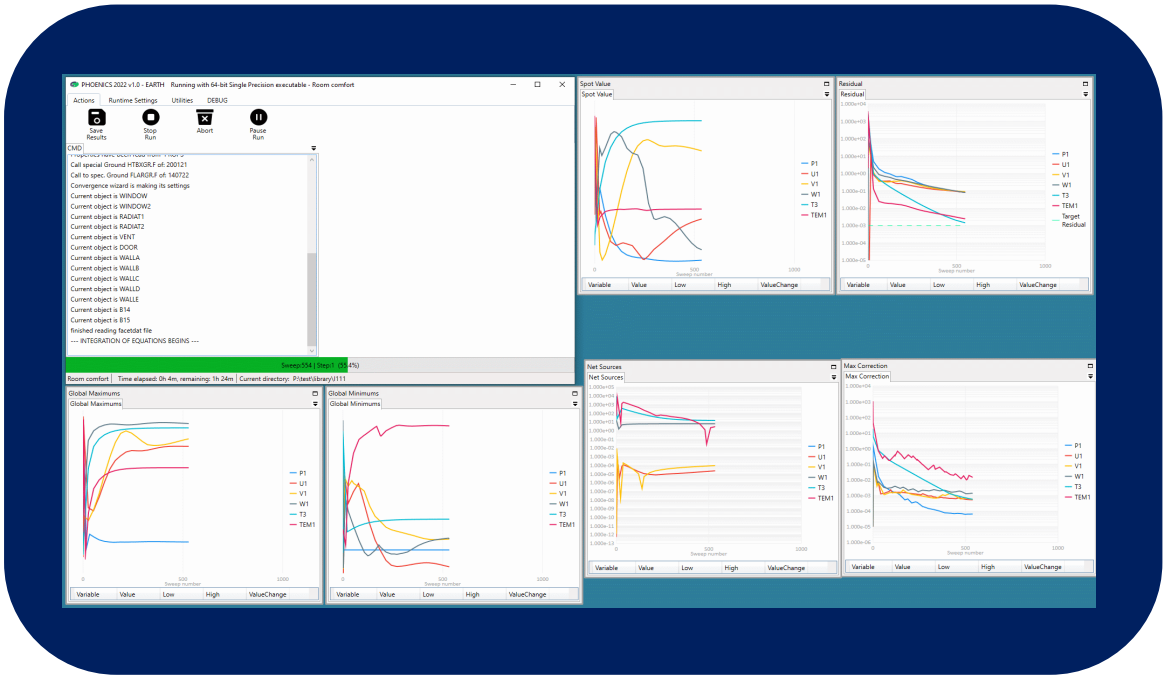

If preferred, they can all be displayed within the main Earth window by changing the docking arrangement:

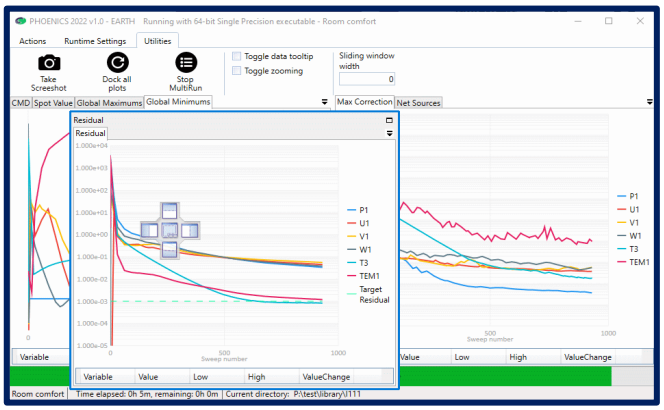

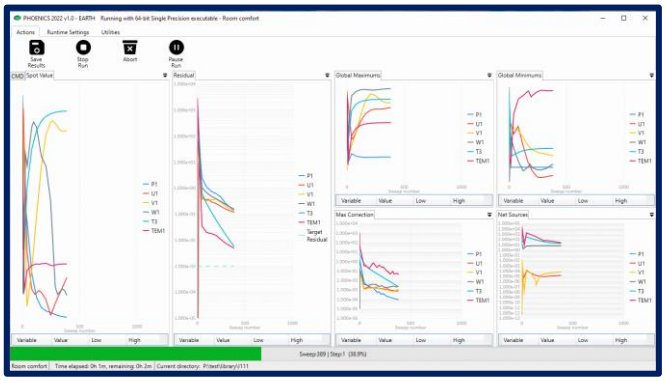

Actions

The ribbon along the top of the window contains the following items, each of which has a 'hover' tooltip:

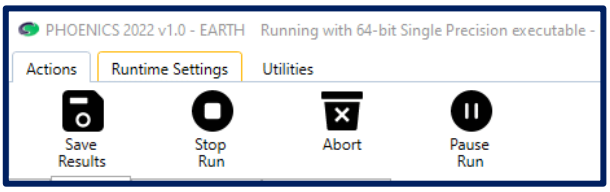

- **Save Results:** brings up a dialog for saving a solution file at the current sweep.
- **Stop Run:** stops the run neatly and saves output files.
- **Abort:** stops the run without saving any output files.
- **Pause Run:** pauses until continue button activated. Interface allows tabs to be rearranged at leisure.

Runtime Settings

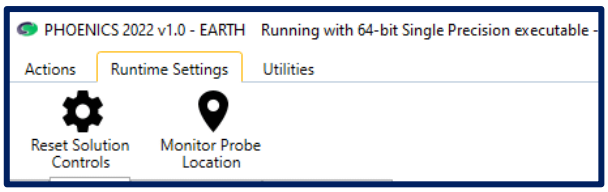

- **Reset Solution Controls** - brings up a dialog for resetting various solution control items.
- **Monitor Probe Location** - brings up a dialog for changing the location of the monitor point.

The solver is paused as long as either dialog is open.

Utilities

- **Take Screenshot:** takes images of each monitor plot. File names will be 'convergence-spot-sweepN.png', 'convergence-residual-sweepN.png', convergence-domainmin-sweepN.png', 'convergence-domainmax-sweepN.png', 'convergence-netsources-sweepN.png' and 'domain-maxcorrection-sweepN.png' where N is sweep (iteration) number.
- **Dock all plots:** automatically puts all un-docked plots back into default positions.
- **Stop MultiRun:** creates the file 'stopmulti', to prevent a multi-run proceeding once the current run finishes.
- **Toggle data tooltip:** displays values by hovering the mouse over any convergence plot:

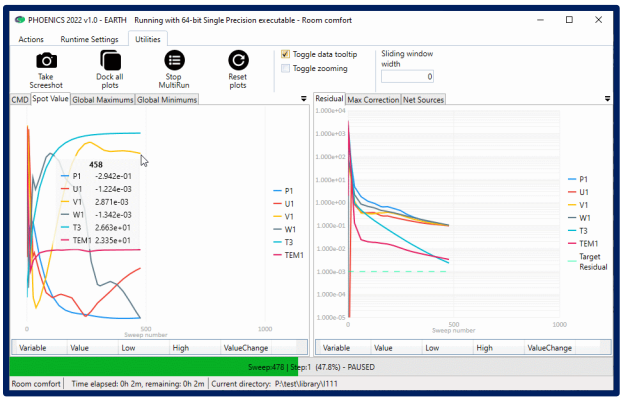

- **Toggle zooming:** when zoom is on left or right mouse buttons can be used to pan the image in any monitor window, and the mouse wheel can be used to zoom in and out. Turning zooming off restores original view.
- **Sliding window width:** when value N>0 is entered into window width box, X axes of graphs show only last N sweeps on a rolling basis. This can be switched from Editor, Options, Solver Monitor Options.

The new convergence monitor introduces a smaller solver delay than the 'classic' one. In the case of very small grids, or transient cases where each step converges in 2-3 sweeps. the 'classic' monitor may be more advantageous.

The 'classic' solver convergence monitor (the GXMONI screen) can be recovered by adding the line:

SPEDAT(SET, GXMONI, CLASSIC, L, T)

to Group 19 of Q1. If the line is absent, or has 'F' instead of 'T' as the last argument, the new style will be used.

This can also be done from within the VR Editor by selecting 'Classic' on the Options-Monitor options dialog.

PHOENICS Simulation of a Phase-Change-Material Battery installed in a Building Climate Tower

by **Peter van den Engel & Michael Malin***

Delft University of Technology, Delft, 2600 GA, The Netherlands: (p.j.w.vandenengel@tudelft.nl)

**Concentration Heat And Momentum Limited (CHAM), London, UK (mrm@cham.co.uk)*

Introduction

The Delft University of Technology and CHAM have recently published a paper entitled "Performance of a Phase Change Material Battery (PCM) in a Transparent Building" [1]. This paper was an outcome of a research project [2] concerned with answering the question as to what extent a combination of low-energy usage and good comfort is possible in the transparent building shown in Figure 1 (a). This building, which is also known as the Co-Creation Centre (CCC) [3], is located at the Green Village on the TU Delft Campus. This fully-glazed building serves not only as an event and meeting centre, but also as research laboratory fully equipped with sensors.

The PCM battery is installed in the climate-control tower attached to this building, as shown in Figure 1(b). This tower provides climatization through a system comprising a heat recovery unit, a battery of PCM plates, and an auxiliary heat pump [4]. While the fans in the climate tower ventilate the building, the heat-recovery unit recovers the waste heat from the air downstream of the building, and the PCM battery buffers the oscillations in temperature of the supply air [4].

One of the aims of climate control is to make use of active-controlled passive-climate features so as to prevent active heating and cooling as much as possible. These passive features include smart controlled solar radiation via the windows for heating, heat recovery, automatically-controlled natural ventilation, and the use of the PCM battery connected to the supply- and return-air handling unit.

(a) Co Creation Centre

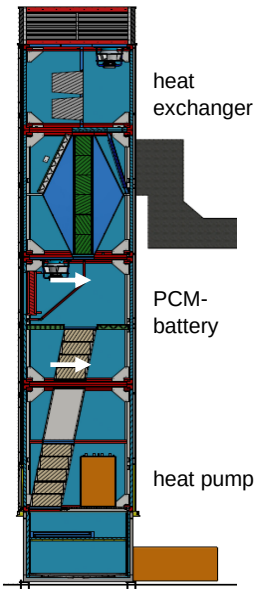

(b) PCM-battery in the climate tower

(c) PCM-panels, temperature sensors are connected on the lowest panel surface.

Figurer 1: Overview of the site, climate tower and PCM-application

The Phase-Change-Material Battery

PCMs store heat by phase transition from solid to liquid when the ambient temperature rises above their melting point; and they release the stored heat when the ambient temperature falls below their freezing point. This cyclic process, which stabilizes the interior conditions of the building, can provide benefits in terms of energy conservation and improving thermal comfort.

The PCM used in the present work is calcium chloride hexahydrate, and it is housed in a high-density-polyethylene (HDPE) rectangular panel, as shown in Figure 1(c). The PCM battery is distributed across 1,170 of these panels, each with dimensions of (height, length, width)=(0.275, 0.57, 0.013) m. The panels are stacked inside the climate tower, as indicated in Figure 1(b). There is an air channel of 4 mm width between each panel, and air is driven through these channels by forced

convection. In the installation, a maximum air flow of 6,000-10,800 m^3/h is possible for sufficient cooling at an occasional high occupancy of 240 people. A peak airflow rate of 10,800 m^3/h equates to a velocity of 2.3 m/s between each PCM panel. The PCM battery adds additional cooling or heating power to building, and can be cooled by night-time ventilation and heated by warm return air.

Physical properties of the PCM are taken as follows: liquidus and solidus temperatures of 23°C and 20°C, respectively; liquid- and solid-phase densities of 1000 kg/m^3; liquid- and solid-phase specific-heat capacities of 2.1 and 1.4 kJ/kgK, respectively; liquid- and solid-phase thermal conductivities of 0.5 W/mK and 1.1 W/mK, respectively; a liquid kinematic viscosity of $9.6.10^{-6}$ m^2/s; and a latent heat of 310 kJ/kg.

CFD Model

A PHOENICS-based transient, three-dimensional CFD-model was developed to simulate the flow and heat transfer within the PCM battery. The CFD model solves the conservation equations for mass, momentum and energy. The battery comprises the liquid and solid regions of the PCM which are housed within solid casings, and these in turn undergo conjugate heat transfer with the air flow in the adjacent channels. The PCM's undergo melting and solidification processes with natural convection in the melt, and they are modelled using the enthalpy-porosity formulation of Voller and Prakash [5], but with the use of an effective specific heat capacity rather than a source term for the treatment of the latent-heat evolution. For this purpose, a linear phase change is employed whereby the effective specific heat $C_{p,e}$ is computed from

$$C_{p,e} = \frac{1}{T}\left[\int_0^T C_p\, dT + (1 - f_s)L\right]$$

where C_p is the mixture specific heat, L is the latent heat and f_s is the solids fraction, which is determined from the Schiel equation:

$$f_s = 1 : T \le T_s \quad \& \quad f_s = 0 : T \ge T_l$$
$$\& \; f_s = \left[\frac{T_l - T}{T_l - T_s}\right]^m : T_s < T < T_l$$

Here, T_s and T_l are the solidus and liquidus temperatures, and the exponent m is taken as unity.

The InForm facility of PHOENICS is used to implement the foregoing phase-change model. The buoyancy forces in the PCM melt are modelled using the Boussinesq approximation, and a Kozeny-Carmen type source term is used to model the flow resistance. The turbulence in the air channels is modelled using the standard k-ε model with equilibrium wall functions. Although the PCM casing is made of HDPE with 0.6 mm thickness, it is modelled as glass with a thickness of 1 mm, so as produce an equivalent thermal conductance.

Computational Details

The solution domain and mesh used for the CFD simulations are shown in Figure 2. This domain considers circa 1/6 of a PCM compartment, and has the dimensions (x, y, z)=(0.57, 0.036, 0.05)m. It consists of one complete panel at the centre, and two half panels on either side. Thus, from left to right in the end elevation of Figure 2 we have 6mm of PCM, 1mm of solid casing, 4mm of air, 1 mm of casing, 12mm of PCM, 1mm of casing, 4mm of air, 1mm of casing, and then 6mm of PCM. This means that there are two air channels of 4mm width on either side of the central panel. The mesh used has 30 cells in the X direction, 36 cells in the Y direction, and 20 cells in the Z direction.

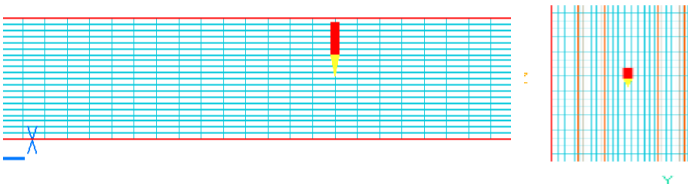

Figure 2: CFD solution domain and mesh

The initial temperature throughout the entire system is 13.5°C, and the sides of the entire system are adiabatic. As will be explained later both the inlet velocity and temperature of the air vary with time, but largely the air enters each channel at 0.31 m/s with a temperature of 25°C. The PHOENICS simulation employs uniform time steps of 5 minutes to cover a simulated time of 24 hours. The InForm facility is used to output a file containing the temporal history of average PCM temperature and solid fraction, the heat transfer rate into the air channels, and the air exit temperatures.

Results and Discussion

The PHOENICS simulations are compared with both on-site measurements and the results produced by a simplified MATLAB-model, which is a transient, one-dimensional lumped-parameter model. However, the outcome of these comparisons has been fully reported elsewhere [1], and so here only the highlights of the CFD simulations are presented and discussed.

Figure 3(a) presents the variation in the measured and predicted PCM average temperature throughout the day. The figure also includes the specified variation in inlet air temperature and velocity. It can be seen that the CFD-model shows an acceptable accuracy to predict the thermal behavior of the PCM, and the differences between the measurements and simulations can be explained in the following way. In the CFD-model, the phase-change energy is considered to be uniform between 20 and 23°C, which leads to lower predicted temperatures at 20–21°C. In reality, the phase-change energy is temperature dependent, as indicated in Figure 3(b), which reveals that the peak phase change is at 22°C.

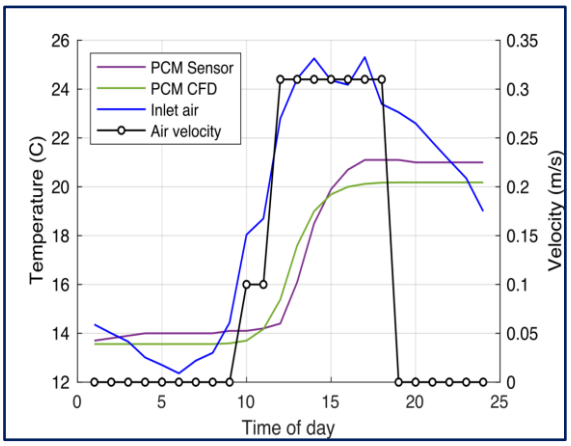

a. Measurements of the temperature compared with CFD-simulations

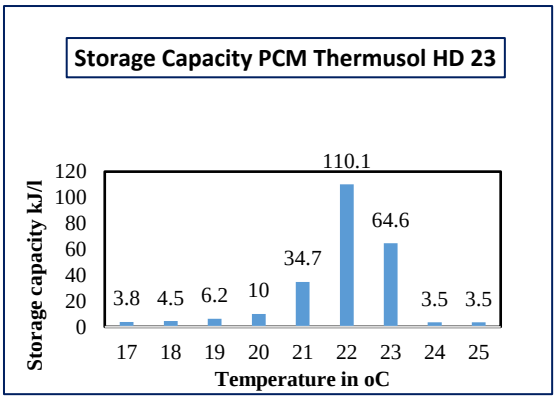

b. Phase-change profile between 20 and 23°C of a PCM-material with an energy content of 172kJ/kg. The present case uses a latent heat content of 310kJ/kg

Figure 3: Measurements, simulations and PCM-characteristics

Temperature contours at the central plane of the PCM panel are shown in Figure 4. Each contour plot is displayed at different times during the time interval 17 to 24 hours. These contours correspond to the night-cooling period of August 10th using air conditions for a peak summer day in Delft. The yellow zone identifies temperatures above 20°C, so one can see the phase-change front (the yellow zone) cooling with time. Buoyancy effects can also be seen in the contours with a larger quantity of warmer PCM mass at the top of the panel, and a colder mass at the bottom. Consequently, the solidification rate inside the PCM is higher at the bottom, while the melting rate is higher at the top of the panel. Figure 4 also highlights that the phase change is not spatially uniform, which brings up the challenge of measuring these temperatures. In reality, the panel is divided into six semi-closed compartments, and so the temperature distribution will differ.

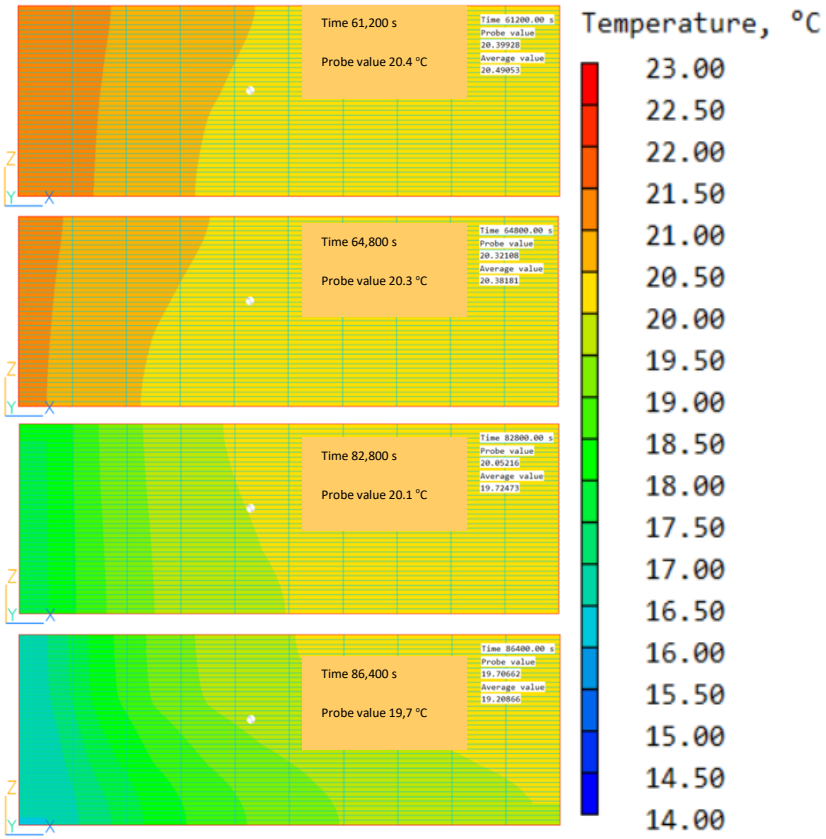

Figure 4: Temperature contours predicted the core of PCM panel, as a function of time.

Conclusions

PHOENICS has been used to simulate successfully the temporal behaviour and performance of a PCM battery. With the present PCM and a phase transition between 20 and 23°C, the building can be cooled or heated in a passive way. Predictions of the effectiveness of heating and cooling of the PCM are possible with CFD, as well as with the simpler MATLAB model in which the PCM is only considered as a solid with a high energy content within the phase change temperatures. The latter, when integrated in a simulation model of the whole building, is able to simulate a whole year in a relative short time [4].

The models showed that there is a limited amount of internal heat available to load the PCM in the heating season and that the required cooling is not high due to effective outside sunshade and night ventilation. However, the savings combined with a smart predictive control are already 37%. Adding PCM panels with a lower phase-change temperature of 17°C is one of the adaptations which will reduce the energy demand even more.

References:

1. Engel, P.J.W van den, Malin, M.R., Venkatesh, M.K, Araujo Passos, L.A. de. Performance of a Phase Change-Material Battery in a Transparent Building. Journal of Fluid Dynamics & Materials Processing. September, Vol. 19, No. 3. (2022).
2. Engel, P.J.W van den, Bokel, R.M.J, Bembrilla E., Araujo Passos, L.A. de and Lucuere, P.G., Converge: low energy with active passiveness in a transparent highly occupied building. REHVA 14th HVAC World Congress, Proc. CLIMA2022, Rotterdam, The Netherlands. (2022).
3. Co-Creation-Centre-and-Nonohouse. https://www.mecanoo.nl/Projects/project/261/Co-Creation-Centre-and-Nonohouse.
4. Araujo Passos, L.A de, Engel, P.J.W. van den, Baldi, S., De Schutter, B., Dynamic optimization of an indoor climate system with latent heat storage, heat recovery, natural ventilation and solar shadings. Energy Conservation and Management. {*Manuscript under review*}. (2022).
5. Voller, V. R., Prakash, C. A fixed grid numerical modelling methodology for convection-diffusion mushy region phase-change problems. International Journal of Heat and Mass Transfer, 30, 709–1719. DOI 10.1016/0017-9310(87)90317-6, (1987).

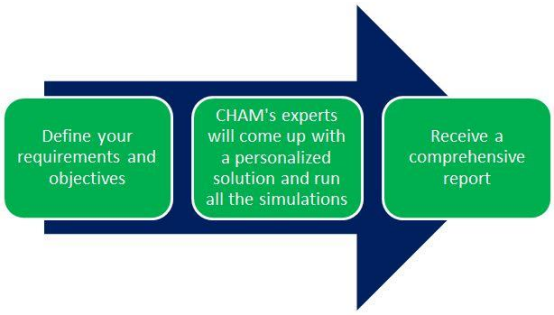

Development of VOF Methods and Surface Tension-Related Forces in PHOENICS for Physical Problems Involving Surfactants with Adsorption/Desorption

Dr J Ouazzani, ArcoFluid France and USA

Introduction

This article reports on the extension of the volume-of-fluid (VOF) method embodied in PHOENICS to handle the Marangoni flows caused by surface-tension gradients at the interface of two phases, usually a liquid and a gas. Such flows can be generated by thermally-induced changes in the surface tension and/or by the introduction of a surfactant, an agent which decreases the surface tension locally, thereby inducing flow away from the region of lower surface tension. Marangoni convection appears in many biological and industrial applications, such as for example welding and pulmonary drug delivery.

Surfactants

In the absence of bulk fluid motion, surfactants adsorb at a two-phase interface to reach an interfacial concentration, Γeq, which is in equilibrium with bulk surfactant concentration *F*. In the presence of bulk fluid motion, the equilibrium is disturbed due to convection, diffusion, and surfactant transport from the bulk resulting in a surfactant concentration distribution, Γ, along the interface. Surfactant effects are twofold: firstly, they change the magnitude of surface tension, resulting in changes to the capillary pressure that drives the instability; secondly, a non-uniform surfactant distribution creates surface-tension gradients which result in surface shear stresses. While surfactants are transferred by convection and diffusion along the interface, they are also transported by adsorption-desorption and diffusion between interface and bulk.

Surface Equation of State

A surface Equation of State (EoS) describes the relationship between interfacial tension σ, and the surfactant concentration at the interface Γ. In the limit of low surfactant concentrations, a linear EoS can be assumed. However, as the interface gets saturated with surfactants, the finite size of the surfactant restricts the maximum amount of surfactant that can be packed at the interface. This maximum surface packing limit is given by Γ_∞ which affects how surface tension changes with surfactant concentration. In addition, surfactants can interact either cohesively or repulsively, which further affects the form of the EoS. For this study, the simplest non-linear EoS accounting for surface saturation effects but no interactions between surfactant molecules, namely, the Langmuir EoS is chosen. The appropriate surface EoS can then be derived from the adsorption isotherm using interfacial thermodynamics.

$$\sigma = \sigma_0 + \mathrm{R}\mathrm{T}\Gamma_\infty \ln\left(1 - \frac{\Gamma}{\Gamma_\infty}\right)$$

Surface Tension developments

The surface-tension terms involve use of the surface normal to the interface for both the curvature (contact line) and Marangoni contributions, whether of thermal or solutal origin. Three alternative approaches have been coded to handle surface tension in both 2 and 3 dimensions, namely the height-function, ALE and MAC method.

In the present study, the ALE method has been used for validation cases; the first of these considers a layer of Silicon oil and air in 2 dimensions to check the development of Marangoni convection. A 6mm layer of air lies on top of a 2mm layer of Silicon oil in a rectangular cavity heated from one side to a temperature of 30°C and held at a uniform temperature of 20°C on the other side of the cavity. Results, shown in Figures 1 and 2, conform to those expected for thermocapillary-driven cavity flow. It is noted the free surface stays quite flat at this amplitude of velocities. The other successful test is for a 3D case of water droplets coalescing in Paraffin oil under a temperature gradient, as shown in Figures 3 and 4. These validation-case results show the ability of the model to treat two- and three-dimensional problems with or without thermocapillary effects.

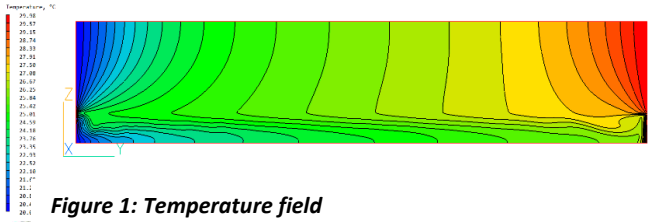

Figure 1: Temperature field

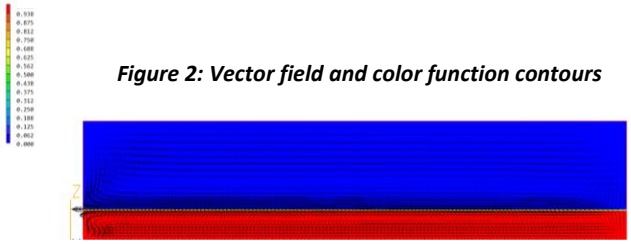

Figure 2: Vector field and color function contours

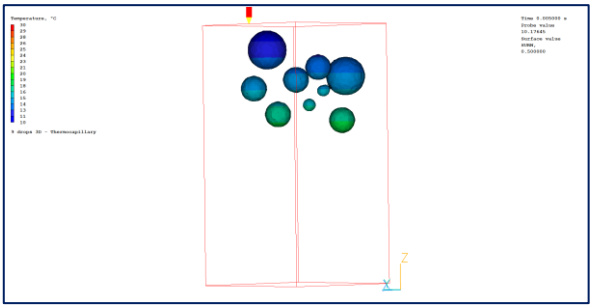

Figure 3: Surface Color function evolution in time colored by temperature

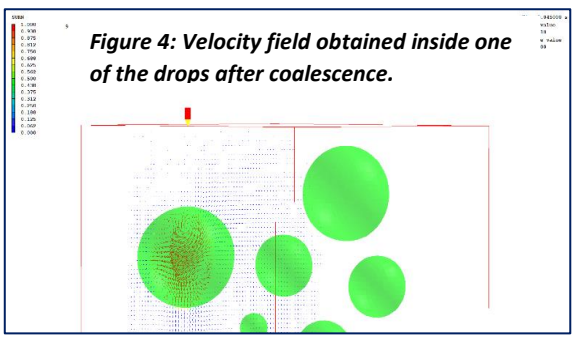

Figure 4: Velocity field obtained inside one of the drops after coalescence.

Surfactant equation of evolution

The changes in concentration of surfactant on a deforming liquid-gas interface are governed by:

$$\frac{\partial \Gamma}{\partial t} + \nabla_s.(\Gamma u_s) + \Gamma(\nabla_s.\mathrm{n})(\mathrm{u}.\mathrm{n}) = D_s\Delta_s\Gamma + \beta_s C_s(\Gamma_\infty - \Gamma) - \alpha_s\Gamma$$

(Stone 1990), where Γ is the mass of surfactant per unit interfacial area, $\nabla_s = (\mathrm{I} - \mathrm{nn}).\nabla$ is the surface gradient operator, $u_s = (I - nn)\_u$ is the velocity along the surface and n is the unit normal to the interface; thus $\nabla_s.n = \kappa$ A, D_s denotes the interfacial diffusivity of surfactants, and β_σ and α_σ are kinetic constants for adsorption and desorption, respectively. For the Laplacian on the surface we can rewrite as follows:

$$\Delta_s = \Delta - \frac{\partial^2}{\partial n^2} - \kappa\frac{\partial}{\partial n}$$

The term $\frac{\partial}{\partial n}$ is similar to $n.\nabla$ and $\frac{\partial^2}{\partial n^2}$ is similar to $n.\nabla(n.\nabla)$ which gives us for: $\Delta_s\Gamma = \Delta\Gamma - n.\nabla(n.\nabla\Gamma) - \kappa n.\nabla\Gamma$

The surfactant equation assuming $\nabla.u = 0$ can be rewritten as

$$\frac{\partial \Gamma}{\partial t} + \nabla.(\Gamma\mathrm{u}) = D_s\Delta\Gamma + \beta_s C_s(\Gamma_\infty - \Gamma) - \alpha_s\Gamma - \Gamma\, n.\nabla u.n - n.\nabla(n.\nabla\Gamma) - \kappa n.\nabla\Gamma$$

$$\frac{\partial \Gamma}{\partial t} + \nabla.(\Gamma\mathrm{u}) = D_s\Delta\Gamma + S_{da} + S_\Gamma$$

$n.\nabla u.n$ is the normal component of the normal derivative:

$$S_\Gamma = -\Gamma n.\nabla u.n - n.\nabla(n.\nabla\Gamma) - \kappa n.\nabla\Gamma$$

$$S_{da} = \beta_s C_s(\Gamma_\infty - \Gamma) - \alpha_s\Gamma$$

This equation form more suitable for numerical treatment.

Numerical Algorithm for Surfactant Equation

This algorithm is original and remains to be published. For the method to be used, we treat the surfactant equation as a combination of advection and diffusion with source terms.

$$\frac{\partial \Gamma}{\partial t} + \nabla.(\Gamma\mathrm{u}) = \nabla.(D_s\nabla\Gamma) + (S_{da} + S_\Gamma)$$

Zero Step:

We start with an initial condition of Γ over a thickness δ on top of the color function interface.

First Step:

We define and compute a new variable $\Psi = \frac{\Gamma - \Gamma_0}{\Gamma_1 - \Gamma_0}$; where Γ_1 & Γ_0 have to be defined as the Max and Min of Γ at the beginning of the timestep.

Second Step:

We compute the following equation:

$$\frac{\partial \Psi}{\partial t} + \nabla.(\Psi\mathrm{u}) = 0$$

This equation is solved explicitly using the VOF – THINC / or VOF – CICSAM method. The value of Ψ should be between 0 and 1. Applying this technic exactly as for the color function ensures that we have the same advective/convective displacement for both functions. This equation gives us: Ψ^{n+1}.

Third Step:

Convert Ψ^{n+1} to $\Gamma^{n+\frac{1}{2}}$ via $\Gamma^{n+\frac{1}{2}} = \Psi^{n+1} * (\Gamma_1 - \Gamma_0) + \Gamma_0$.

Fourth Step:

Solve the diffusion equation for Γ using $\Gamma^{n+\frac{1}{2}}$.

$$\nabla.(D_s\nabla\Gamma^{n+1}) + (S_{da} + S_\Gamma)^{n+1} + \frac{1}{\Delta t}(\Gamma^{n+\frac{1}{2}} - \Gamma^{n+1})$$

This resolution is made over the thickness δ. To ensure that, we multiply all the equation by δ_Γ which value is one over the thickness δ and zero elsewhere. This diffusion equation is solved implicitly using the available PHOENICS solver with source terms easily introduced in the equation through linearized terms sources.

Fifth Step:

We compute $\Psi^n = \frac{\Gamma^{n+1}-\Gamma_0}{\Gamma_1-\Gamma_0}$ with new Γ_1 & Γ_0.

We go to second step.

Note: to estimate the zone under which the surfactant is present, we define the following variable:

$$\Omega = 4\tilde{C}(1 - \tilde{C})$$

$$\tilde{C} \text{ is the smoothed color function}$$

IF $\Omega > 10^{-6}\ then\ \delta_\Gamma = 1\ else\ \delta_\Gamma = 0$ we are then left with describing correctly the source terms arising in the second member of the equation. The term S_{da} is straightforward and is treated implicitly as well as linearized depending on the sign of $\beta_s\ and\ \alpha_s$. For the term S_Γ an Adams-Bashforth 2nd order scheme for the time discretization has been implemented.

Surfactant Bulk Equation

Beside the surfactant surface equation, the bulk concentration of the surfactant is needed. The bulk surfactant concentration *F* is governed by the advection-diffusion equation

$$\frac{\partial F}{\partial t} + \nabla.(Fu) = D_F \Delta F$$

where F is the surfactant bulk concentration and, D_F is surfactant diffusion coefficient in the bulk. This equation is solved as follows

$$\frac{\partial F}{\partial t} + \nabla.(Fu) = D_F \nabla.(\nabla F) + S_F + S_{dabulk}$$

$$S_F = \begin{cases} 10^{20}(0 - F_P)\ outside\ bulk \\ 0\ inside\ the\ bulk \end{cases}$$

Fp being the value of F at the centre of the cell, the diffusion coefficient is domain dependent.

S_{dabulk} is the source term representing the adsorption/desorption in/out of the bulk.

The boundary conditions are incorporated for this equation as a volumetric term source. In this way we can treat both sides of the surfactant, inside the liquid bulk and in the surrounding bulk. Setting the equations in such a way enables us to use the PHOENICS code solvers and discretization.

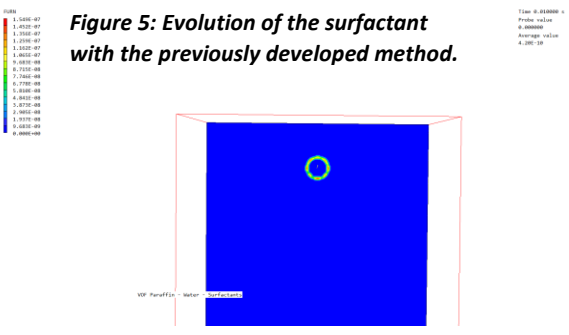

Figure 5: Evolution of the surfactant with the previously developed method.

In the following are the results for a 3D case.

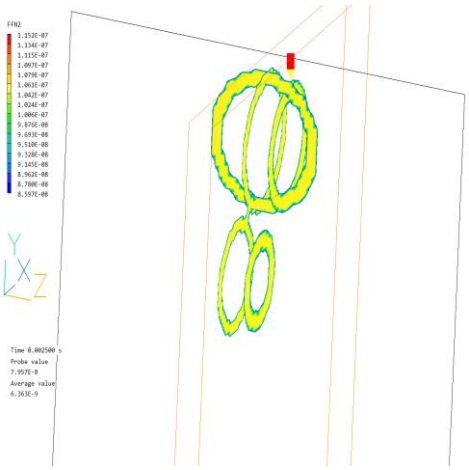

Figure 6: Evolution of the surfactant with the previously developed method in 3D.

References:

1) Stone, HA. (1990) A simple derivation of the time-dependent convective-diffusion equation for surfactant transport along a deforming interface. Phys. Fluids A 2, 111-112.

2) Stone HA, Leal, LG. (1990) The effects of surfactants on drop deformation and breakup. J. Fluid Mech. **220**, 161-186.

3) Zimmermans LE, Lister JR., The effect of surfactant on the stability of a liquid thread J. Fluid Mech. (2002), vol. 459, pp. 289-306.

4) Eggleton CD, Stebe KJ. (1998) An adsorption-desorption controlled surfactant on a deforming droplet, J.Colloid Interface Sci. 208, 68.

5) Muradoglu M, Tryggvason G. (2008) A front-tracking method for computation of interfacial flows with soluble surfactants, J. Comp Phys. 227, 2238.

6) Tasoglu S, Demirci U, Muradoclu M. The effect of soluble surfactant on the transient motion of a buoyancy-driven bubble, Physics of Fluids **20**, 040805 (2008); doi: 10.1063/1.2912441.

7) Scriven LE, Sternling CV. (1960) The Marangoni effects. *Nature* 187, 186–188.

8) Jian-Jun Xu, Hong-Kai Zhao, (2003) An Eulerian Formulation for Solving Partial Differential Equations along a Moving Interface, *J Scientific Computing, Vol. 19, Nos. 1–3.*

9) James A.J, Lowengrub J. (2004). A surfactant-conserving volume-of-fluid method for interfacial flows with insoluble surfactant. J Comp Physics, 201(2), 685–722.

10) Li Z, Lai M-C. (2001). The immersed interface method for the Navier-Stokes equations with singular forces. J Comp Physics, 171, 822–842.

11) Xu J-J, et al (2006). A level set method for interfacial flows with surfactants. J Comp Physics, 212(2), 590–616.

12) Teigen KE, et al A diffuse-interface method for two-phase flows with soluble surfactants, J Comput Phys. 2011 January 20; 230(2): 375–393. doi: 10.1016/j.jcp.2010.09.020.

Anti-icing of the Helicopter Deck in Arctic Conditions.

Arne Holdo, Professor Emeritus, UIT, Narvik, Norway

The Helicopter deck is frequently the main crew escape route for fixed Offshore structures, Drilling Rigs and FPSO (Floating Production Storage and Off-loading) units. The environmental conditions on Helicopter decks are therefore subject to international regulations and National Standards.

When such units are situated or relocated to areas experiencing arctic weather conditions, special care must be taken in design and preparation of the Helicopter decks as well as the escape routes to these decks. The Norwegian Standard for Helicopter decks on offshore installations (NORSOK C-004:2019) states in general that Computational fluid dynamics (CFD) analysis should be used in the design of Helicopter decks for Offshore structures.

Exposure to Arctic conditions means additional weather hazards to those found in more temperate regions have to be studied. One concern is the conditions on the surface of the helideck which should be skid-proof in all directions, and under all conditions. This should be the case for both helicopters and personnel, but at low arctic temperatures both snow and ice can be a hazard.

In terms of ice conditions, heat transfer and heat tracing of the helideck is therefore a further part of the CFD study when examining helidecks in arctic conditions. Wind, local velocity and turbulence conditions are also important for the design parameters so that any heat tracing rates and insulation layer thicknesses can be determined so that detrimental conditions do not take place for either helicopter and personnel.

An example test was carried out at a design temperature of -15C with a wind speed of 10 m/s at a reference height of 10 m above sea level. Standard aluminium heat transfer properties were used whilst turbulence due to the high Reynolds number was modelled using the well-known k-ε two-equation, eddy-viscosity turbulence model.

The first test was carried out with only the aluminium helideck properties and maximum heat tracing rate. The temperature distribution is seen in Figure 1 and it is demonstrated that the deck surface never reaches +4 C which is the minimum requirement for an anti-icing helicopter deck. This is more clearly seen in Figure 2 showing centreline temperatures.

A second test was carried out with an insulated lower part of the helicopter deck. The results from this test are shown by Figure 3 and 4 which demonstrates that the deck temperatures of the insulated model helicopter deck are largely above 4 C, suggesting that insulation of the deck is necessary and that heat tracing on its own is not adequate.

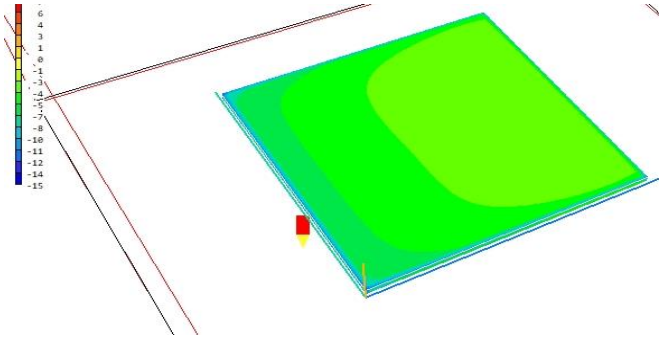

Figure 1 Temperature contours on non-insulated helicopter deck model.

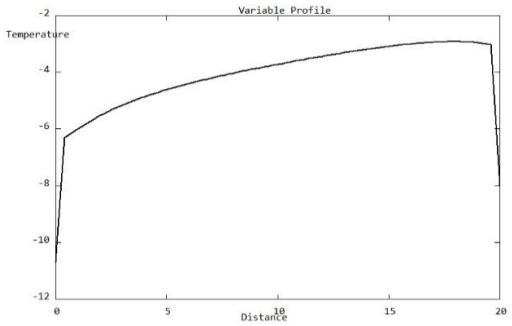

Figure 2 Centre line deck temperature on the non-insulated helicopter deck model.

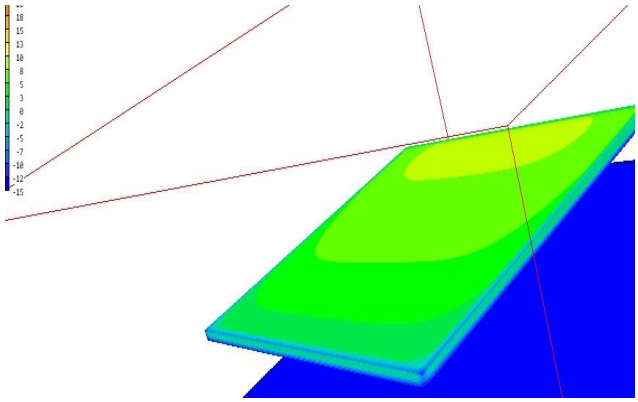

Figure 3 Temperature contours of the insulated helicopter deck model.

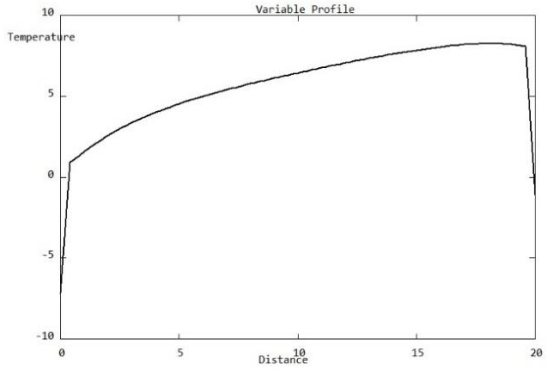

News from CHAM Agents:

ACFDA, Dr Vladimir Agranat, Canada & USA

Applied Computational Fluid Dynamics Analysis (ACFDA), CHAM's agent since 1998, has been promoting PHOENICS/FLAIR software sales, CFD training and consulting services in Canada, USA, Israel and Kazakhstan for general and more specific applications such as wildfire spread and its interaction with urban structures, virus transmission and mitigation, pollution dispersion, hydrogen production, etc. These particular PHOENICS applications are described on the following webpages:

1. *Physics-based CFD modeling of wildfire spread and its interactions with urban structures (www.acfda.org/results/Agranat_Perminov_EMS_2020_Published.pdf);*
2. *CFD modeling of virus transmission in built environments for health and safety analyses (https://www.acfda.org/results/Virus_Spread_CFD_Study.pdf);*
3. *CFD modeling of two-phase plumes (https://www.acfda.org/docs/Paper_ICONE22-30010_Agranat_et_al.pdf);*
4. *Modeling of electrolysis stacks for hydrogen production optimization (https://www.acfda.org/docs/ASME2006-98355.pdf);*
5. *Modeling of gas releases and dispersion for environmental and safety analyses (https://www.acfda.org/results/2014_ASSE-MEC_CFD.pdf).*

Additional information is available from info@acfda.org

ArcoFluid France, Dr J Ouazzani and ArcoFluid Consulting LLC (Florida, USA), Mr Z Ouazzani

Dr Jalil Ouazzani (below left), will focus on working exclusively on ArcoFluid in France and French-speaking countries to develop activities related to PHOENICS & FLAIR software. Mr Zaim Ouazzani (below right) becomes the manager of ArcoFluid Consulting LLc and will take care of the North American market concerning the sales and follow up of PHOENICS and FLAIR software.

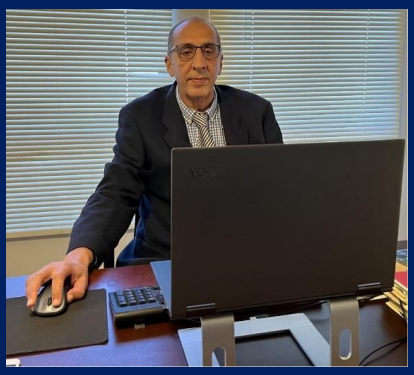

Dr Jalil Ouazzani is involved in two ESA projects, one on emulsions and another on droplet evaporation/condensation phenomena: 2019-2023 MAP project "Emulsion Dynamics and Droplet Interface – EDDI" (ESA); 2019-2023 "Convection and Interfacial Mass Exchange" (EVAPORATION), (ESA)

Dr Ouazzani will present the development work of VOF models done in PHOENICS with the collaboration of University of Marseille at the two days ESA meeting in Parma (Italy) (November 3 - 4 2022).

News from CHAM Agents, continued:

Dr Frank Kanters, of Coolplug, sent us the following sad item. As Frank says, Frank Zimmerman will be sorely missed. He used PHOENICS over years for diverse applications; he was part of the "PHOENICS family".

Frank Kanters

Dr Frank Kanters, Coolplug, Benelux Area

"Last July a very loyal PHOENICS user from Germany, Dipl.-ing Frank Zimmermann passed away at the age of 85. Until a few weeks before his death I was in contact with him about the use of PHOENICS to climatize a museum. In 2020 he worked on a project to make visiting concerts possible in COVID time by simulating the flow of aerosols in a concert hall with PHOENICS. This has led to a publication in Nature Communications.

Frank Zimmermann was born in Dresden, where he survived the heavy bombardment in 1945, and fled to West Germany just before the completion of the Berlin Wall in 1961. Here he founded the engineering bureau Zimmermann and Becker together with his partner. He was always one of the first when it came to using modern engineering tools such as CAD and CFD. He has also been involved in writing guidelines for the HVAC section of the German engineering association VDI. He will be missed."

News from CHAM:

PHOENICS-2022 (as described in the Summer Newsletter) is now available. The latest version can be obtained from CHAM and can be accessed, on the Cloud. This option allows pay-as-you go access to a powerful CFD tool which can be run on a variety of virtual machines as offered by the Microsoft Azure marketplace: https://www.cham.co.uk/_docs/pdfs/phoenics_docs/PHOENICS-OTC2021.pdf.

Send your memories of Brian Spalding to newsletter@cham.co.uk for inclusion in the next Newsletter: DBS at 100.

Contact Us:

CHAM provides reliable, cost effective, and proven, software solutions, training, technical support and consulting services. To see how we can help with your needs please give us a call on +44 (20) 89477651 or email us on sales@cham.co.uk. Our website is www.cham.co.uk. For PHOENICS on the Cloud (Azure services) please contact phoenics.cloud@cham.co.uk or call us. We are on the following social media:

Concentration Heat and Momentum Limited (CHAM)
Bakery House, 40 High Street
Wimbledon Village
London SW19 5AU, England